

# EFFECT OF HALOGENS ON THE STRUCTURAL AND ELECTRONIC PROPERTIES OF DIPHENYL- DIKETOPYRROLOPYRROLE AND ITS DERIVATIVES

Hindreen A. Ibrahim a,  
Salah M. A. Ridha b,  
Najlaa Ozaar Hasan c

A Basic Sciences Branch, College of Dentistry, University of Kirkuk, Iraq

B Department of Physics, College of Science, University of Kirkuk, Iraq

C Department of Physics, College of Girls Education, University of Kirkuk, Iraq

handarina.ibrahim@uokirkuk.edu.iq, salahygmuroglu@uokirkuk.edu.iq,

najlaozar@uokirkuk.edu.iq

## Abstract

In the present study, Structural, UV spectroscopic properties and quantum chemical calculations have been performed on theoretical study of the diphenyl-diketopyrrolopyrrole with its derivatives (chlorodiphenyl-diketopyrrolopyrrole, bromodiphenyl-diketopyrrolopyrrole and fluorodiphenyl-diketopyrrolopyrrole) were studied. Using the DFT/B3LYP/6-311G (d,p) level of theory in the gas phase, the compounds' ground state geometries have been optimised. The assigned chemical structure of molecules was confirmed using IR spectroscopic technique. The UV-Vis spectral properties, maximum wavelength, energy and oscillator strength of three compounds were predicted by the TD-DFT approach. The extracted molecular structure has served as the basis for geometric optimisations. The structural and geometric characteristics were computed, and theoretical results were compared to experimental X-ray values obtained from the literature. The computationally calculated structural and geometric characteristics correlate well with the experimentally acquired x-ray values that documented from literature. The effects of the halogen substituent on the characteristic diphenyl-diketopyrrolopyrrole bands in the UV-visible spectral are discussed. In addition, Chemical reactivity descriptors on a global scale, such as frontier molecular orbital analysis, were used to the compounds' optimal structures in order to address their reactive qualities.

**Keywords:** Diphenyl-diketopyrrolopyrrole, DPPs, DFT, Geometry, Energy gap, global reactivity descriptors.

## Introduction

The shortage of fossil fuels and the increasing demand for energy have prompted people to develop new types of clean and sustainable energy [1][2]. In recent times, researchers have observed significant advancements in organic semiconductors, which provide numerous advantages such as flexibility, reduced cost, facile synthesis, scalability, and decreased weight

[1][3][4]. Diketopyrrolopyrrole (DPP), out of all the organic semiconductors that have been documented, has demonstrated remarkable efficacy as a fundamental component in the fabrication of high-performance functional materials applicable to a diverse array of electronic devices [5]. Diketopyrrolopyrrole (DPP) discovered in 1974 by Farnum et al [6], and had not been extensively utilized until Iqbal and his colleagues put forth a comparatively rational synthetic mechanism, until after 10 later. Subsequent to its commercial introduction in 1986 under the name C.I. Pigment Red 255, diphenyl-DPP was rapidly followed by a succession of analogs featuring various substitutes (henceforth referred to as DPPs), which amassed substantial market shares in the pigment industry [7]. Subsequently, DPP gained extensive use as a pigment in inks, as well as in paints for the purpose of coating. Although DPP-based conjugated compounds were first described in 1993, their application as semiconductors in organic electronics did not become widespread until 2008. This was the year that Nguyen, Janssen, and Winnewisser successfully synthesized DPP-based semiconductors that could be processed in solution for usage in OFETs and OPVs. Since 2008, Diketopyrrolopyrrole (DPP) has been acknowledged as a very promising conjugated building block for the fabrication of high-performance semiconducting materials used in a wide range of electronic devices [8]. The planar structure of an organic dye has been demonstrated to make it a promising option for photothermal therapy (PTT) due to its favourable photostability, strong fluorescence, exceptional molar absorption coefficient, and convenient modifiability [9], possesses exhibits distinctive characteristics, including excellent conjugation, strong electron-drawing capability, thermal and photostability stability, and a high quantum efficiency for fluorescence [10]. In addition to its low-bandgap characteristics and the ability to tune energy levels appropriately, the fused highly planar Diketopyrrolopyrrole (DPP) unit is capable of facilitating considerable intermolecular  $\pi$ - $\pi$  interactions, which in turn improves the mobility of charge carriers [11]. The incorporation of different monomeric units (either donor or acceptor) with DPP enables precise manipulation of the energy levels of (HOMO) the highest occupied molecular orbital and lowest unoccupied molecular orbital (LUMO). By manipulating these factors, the hole mobility of p-type materials has surpassed  $10 \text{ cm}^2 \text{ V}^{-1} \text{ s}^{-1}$ , whereas the electron mobility of n-type semiconductors has achieved over  $1 \text{ cm}^2 \text{ V}^{-1} \text{ s}^{-1}$  [5]. The aromatic ring substituents play an important function in the conjugate system, influencing the maximum absorption and emission wavelengths of the entire molecule [12]. Due to their high electron mobility, DPPs have garnered significant attention in the field of energy, leading to increased interest [8]. From their accidental synthesis in the 1970s to their subsequent widespread use as a high-quality pigment twenty years later, and now to their current status as a promising new energy solution, Diketopyrrolopyrrole (DPPs) have been blessed with ever-evolving values and concepts. The energy area has received a lot of attention and resources thus far [7]. However, the primary purpose of DPPs, which is to enhance our lives with vibrant hues, is being disregarded. The chromophore of DPPs consists of a central core composed of two fused pyrrolidone rings, as indicated by its name. The most basic derivative of this kind, diphenyl-DPP, has a maximum absorption at 538 nm in solid state, resulting in a red color. Other derivatives within the DPP

family can exhibit either a violet or orange color variation, depending on whether their absorption is shifted towards the blue or red end of the spectrum. This shift is caused by the electron donating or withdrawing impact of conjugation. The distinctive characteristics of DPPs mostly arise from the  $\pi$ - $\pi$  stacking interactions between aromatic rings and the hydrogen bonding facilitated by lactam units. DPPs possess a robust intermolecular connection that grants them an exceptionally elevated lattice energy [7].

because to their strong fluorescence properties and exceptional stability [1]. Small molecules derived from DPP have found extensive use in a variety of organic electronic devices over the past few decades [9]. These devices include sensing and bio-imaging [13], organic field-effect transistors [14], organic solar cells [15], ambipolar transistors, dye-sensitized organic solar cells [16], and bulk heterojunction solar cells (BHJ) [17], organic light emitting diodes (OLEDs) [16], memory devices, photodetectors [5], organic light emitting diodes [18], organic photovoltaics (OPVs) [19], fluorescent sensors [20], and optical imaging contrast agents. Fluorescent probes based on DPP have been created for a range of analytes [20] including thiols, reactive oxygen species, anions, cations, pH, H<sub>2</sub>, and CO<sub>2</sub> [21], two-photon absorption [22], gas detectors, solid-state dye lasers, [23], and chemical sensors [24]. Plus, DPP derivatives' unique characteristics have led to their remarkable PDT and PTT efficacy in cancer therapy [20], partly due to the synthetic capabilities that allow for the modification of their molecular characteristics to create materials with unique functionalities. Originally, Ciba-Geigy created their synthesis and made the compounds available for sale as automotive pigments [13]. High-performance pigments derived from DPPs are widely used [25]. The compounds have vivid colours (varying from yellow-orange to red-violet) and are extremely resistant to light, heat, chemical, and climate impacts [23]. Additionally, in normal pigment molecule terms, their very low  $M_r$  makes certain of their physical features, such high melting temperatures, unusual. Incorporating (DPP) units into different materials, such as polymers, has been found to have beneficial effects [26], polymer-surfactant complexes, oligomers and dendrimers [25], resulting in intensely variegated and photoluminescent [27], and electroluminescent materials [28]. Solubility is a crucial factor in the fabrication of any device, whether it is in form of thin film consisting of Diketopyrrolopyrrole (DPP) or involves the integration of the Diketopyrrolopyrrole (DPP) unit into a supporting matrix. Diketopyrrolopyrrole (DPP) compounds exhibit limited solubility in most commonly used solvents. Although this characteristic is advantageous for some applications, the ability to dissolve these compounds would enable to use of solution-based methods such as drop-casting, spin-coating, and inkjet printing for the fabrication of DPP-based devices [25].

In the present study, the Optimized geometry, Optical properties and Chemical Description of highest occupied molecular orbital (HOMO) and lowest unoccupied molecular orbital (LUMO) orbital positions required for effective charge transfer, etc, of diphenyl-diketopyrrolopyrrole and its derivatives using density functional theory (DFT) method Hybrid three-parameters Lee-Yang-Par (B3LYP) exchange correlation in combination with 6-311G(d,p) basis set have been studied. None of the compounds has been studied experimentally, but the experimental data of DPP without phenyl groups was obtained [29]. The occurrence of quantum chemical

investigations on these compounds is notably infrequent, the obtained results are discussed and compared with similar literatures of the studied molecules.

## 2. Results and discussions

### 2.1 Optimized geometry

The geometry optimized of all four compounds based on quantum chemical computations using density functional theory (DFT), hybrid three-parameters B3LYP exchange correlation in combination with 6-311G(d,p) basis set. No instances of imaginary frequencies were observed following the diagonalization of the Hessian matrix, so validating the authenticity of the computed geometries as genuine minima on the hypersurfaces of the ground state. The confirmation of these minima as absolute minima in relation to phenyl rotations was obtained through the optimisations conducted using differently rotated initial geometries. The calculations for the single point energy of the ground state were performed on the geometries obtained from the optimization technique. Only for (DPP) are available experimental X-ray structures [29]. The essential calculated bond lengths and valence angles are presented in Tables 1 and 2. The computed geometric analysis of diphenyl-diketopyrrolopyrrole and its derivatives accurately predicts consistent bond lengths in phenyl rings and alternating bond lengths in heterocycles. Nevertheless, it is unfeasible to quantitatively measure the disparities between the calculated bond lengths and the experimental values using the literature [29]. In fact, the computed values differ more than  $0.03 \text{ \AA}$ . In general, the computed geometry exhibits a higher degree of proximity to SAPDES01 [29]. The two benzene rings are regular hexagons with bond lengths that fall between that of a single ( $1.3958$ ) and double ( $1.3961$ ) bond. This is consistent with the usual values reported in the literature for one bond ( $1.54$ ) and two bonds ( $1.33$ ) [30], since the bond lengths for the two varied ( $0.144$ ) for single and ( $0.066$ ) for double, and the C-H bond lengths between  $1.0827$  and  $1.0841 \text{ \AA}$  is in agreement with [31] between  $1.0853$  and  $1.0870 \text{ \AA}$ , as they differ  $0.0026$ - $0.0029 \text{ \AA}$ . The interatomic distance within the diketopyrrolopyrrole ring are not equal the average value for C=N bond lengths of (DFT) is  $1.28 \text{ \AA}$ , and these values show the C=N bond lengths average value significantly longer than the normal C=N double bond ( $1.22 \text{ \AA}$ ) [32]. The C1=O10 bond lengths is  $1.1999 \text{ \AA}$  (DFT) and the experimental  $1.230 \text{ \AA}$  [29] has the differ more than  $0.03 \text{ \AA}$ . Figure 2(a) illustrates the optimised molecular structure of diphenyl-diketopyrrolopyrrole derivatives, with atom numbering provided. Figure 2(b) displays the crystal structure produced for these compounds, wherein X represents chlorine, bromine, or fluorine. The optimised structural parameters of chloro, bromo, and fluoro-diphenyl-diketopyrrolopyrrole were determined using the density functional theory (DFT) method using the B3LYP functional and the 6-311G(d,p) basis set. The atom numbering scheme provided in Figure 2 (a) was used during the calculations.

The C-C bond lengths lie between  $1.3874$ - $1.4094 \text{ \AA}$  (DFT),  $1.381$ - $1.387 \text{ \AA}$  (XRD) for phenyl ring. In the phenyl ring the bond lengths of C-C lie from  $1.3853$ - $1.4081 \text{ \AA}$  (DFT),  $1.373$ - $1.391 \text{ \AA}$  (XRD). In the phenyl ring the C-C bond lengths are lie in range  $1.3852$ - $1.4094 \text{ \AA}$  (DFT),  $1.372$ - $1.394 \text{ \AA}$  (XRD), for chloro, bromo and fluoro- diphenyl-diketopyrrolopyrrole respectively [33].



In this study, the C-Cl bond length is 1.7549Å for phenyl ring, which is in agreement with literature 1.7637Å [34]. The C-Br bond length is 1.9132Å for phenyl ring, which is in agreement with literature 1.9237Å [35]. The C-F bond length is 1.348Å for phenyl ring, which is in agreement with literature 1.350Å [33]. At C18 position, the bond angles are, C14-C18-C16 = 122.1°, C14-C18-F31 = 119.08°, and C16-C18-F31 = 118.7°, which is in agreement with literature 122.8°, 118.6°, 118.6° respectively [33]. At C18 position, bond angles are, C14-C18-C16 = 121.04°, C14-C18-Br31 = 119.5°, and C16-C18-Br31 = 119.3°, which is in agreement with similar 123.5°, 119.1°, 117.3° respectively [35]. At C18 position, the bond angles are, C14-C18-C16 = 121.06°, C14-C18-Cl31 = 119.5°, and C16-C18-Cl31 = 119.3°, which is in agreement exactly with literature 121.5°, 119.3°, 119.3° respectively [33]. The theoretical values show that the majority of the optimised bond lengths are greater than the experimental values. This overestimation can be explained by fact that the theoretical calculations for isolated molecules in gaseous phase and the experimental data for molecules in solid form. Several writers have provided explanations for the alterations in bond length of the C-H bond upon substitution, particularly when the substituents possess electron-withdrawing properties such as (Cl, F, Br, etc.). These changes are attributed to modifications in the charge distribution on the carbon atom within the benzene ring [33]. The carbon and hydrogen atoms in the benzene ring are connected by a sigma bond, denoted as  $\sigma$ -bond. The introduction of a halogen atom as a substituent result in a decrease in electron density at the carbon atom. Consequently, the introduction of chlorine (Cl), bromine (Br), or fluorine (F) at the 18th carbon (C) atom, which shares its p electron with the ring, induces alterations in the bond lengths and bond angles inside the aromatic ring. It is well-established that DFT approaches consistently produce too-long predictions for bond lengths, especially for C-H bonds [33]. C-H bond lengths have an experimental value of 0.93Å [36], but their theoretical value is greater than 1 Å. For three compounds, the obtained C=C bond lengths lie in the range 1.3853-1.4094Å. However, the experimental X-ray diffraction values for C=C bond lengths range between 1.372 and 1.390 Å [29].

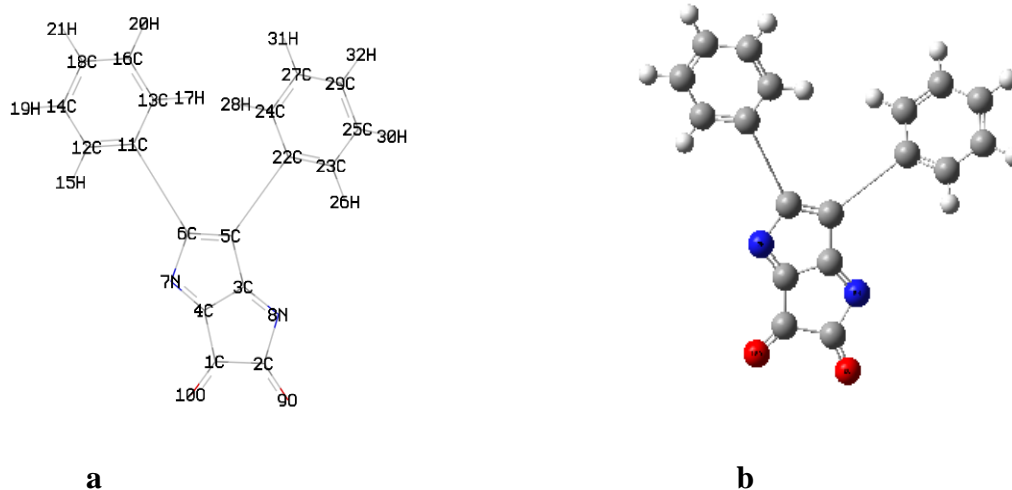
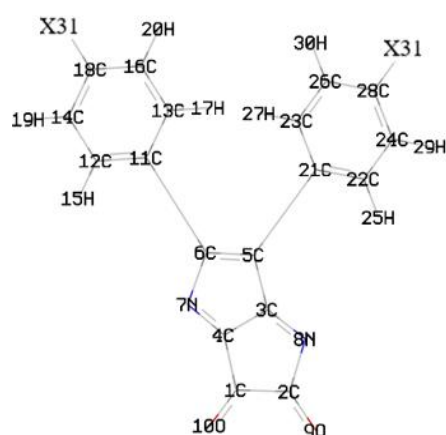
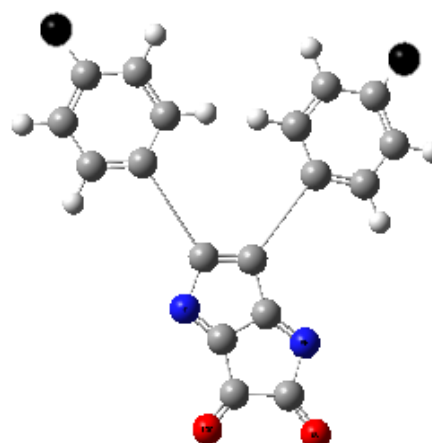


**Fig. 1. (a)** The atoms numbering and the theoretical geometry of the diphenyl-diketopyrrolopyrrole. **(b)** Compounds' molecular geometry with atom numbering where (gray, white, blue, red and black is the carbon C, hydrogen H, nitrogen N and oxygen O) respectively.



a



b

**Fig. 2.** (a) The atoms numbering and the theoretical geometry of the diphenyl-diketopyrrolopyrrole derivatives. (b) Compounds' molecular geometry with atom numbering where (gray, white, blue, red and black is the carbon C, hydrogen H, nitrogen N, oxygen O and X= chlorine Cl and bromine, Br, fluorine F) respectively.

**Table 1.** The ground state energy, bond lengths and bond angles are calculated by DFT/B3LYP with 6-311G(d,p) and experimental data [29] of diphenyl-diketopyrrolopyrrole.

Bond length (Å°)	DFT/B3LYP /6-311G(d,p)	Exp. [29]
C1-C4	1.4746	1.442
C3-C4	1.4818	1.421
C3-C5	1.45	1.383
C6-N7	1.4602	1.373
C4-N7	1.2798	1.409
C1-O10	1.1999	1.230
C6-C11	1.4581	1.456
C11-C12	1.4082	1.390
C11-C13	1.4082	1.405
C12-C14	1.3893	1.395
C13-C16	1.387	1.386
C18-C14	1.3932	1.359
C16-C18	1.3965	1.397
Bond angles (Degrees)		Exp. [29]
C4-C3-C5	105.6785	108.8
C5-C6-N7	112.7064	107.3
C4-N7-C6	105.3521	112.0
C2-N8-C3	106.158	104.2
C1-C4-C3	106.0466	107.7

**Table 2.** The parameters theoretical geometric of chloro, bromo and fluoro-diphenyl-diketopyrrolopyrrole bond lengths in Angstrom (Å), bond angles and dihedral angles in degrees (°).

Bond length (Å)	6-311G(d,p)/B3LYP	Bond length (Å)	6-311G(d,p)/B3LYP		
			X= Cl	X= Br	X= F
C11=C12	1.4082	C12=C11	1.4081	1.4079	1.4094
C13-C11	1.4082	C13-C11	1.4079	1.4078	1.4091
C14-C12	1.3893	C14-C12	1.3876	1.3882	1.3873
H15-C12	1.0813	H15-C12	1.0812	1.0813	1.0811
C16=C13	1.387	C16=C13	1.3853	1.386	1.3852
H17-C13	1.0814	H17-C13	1.0813	1.0814	1.0811
C18=C14	1.3932	C18=C14	1.3917	1.3921	1.3874
H19-C14	1.0837	H19-C14	1.0821	1.082	1.0826
C18-C16	1.3965	C18-C16	1.3951	1.3956	1.3908
H20-C16	1.0838	C16-H20	1.0821	1.082	1.0826
C18-H21	1.0841	C18-X31	1.7503	1.9086	1.3442
Bond angles (Degrees)		Bond angles (Degrees)			
C12-C11-C13	118.657	C12-C11-C13	118.3742	118.3713	118.4963
H14-C12-C11	120.5372	C14- C12-C11	121.005	121.0158	120.9763
H15-C12-C11	118.8633	H15-C12-C11	119.0094	119.0144	118.8972
H15-C12-C14	120.5986	H15-C12-C14	119.9848	119.9688	120.1254
C16-C13-C11	120.4365	C11-C13-C16	120.9251	120.9495	120.8808
H17-C13-C11	119.9265	C11-C13-H17	120.1266	120.1284	120.0168
H17-C13-C16	119.6273	C16-C13-H17	118.9363	118.9104	119.0915
C12-C14-C18	120.1882	C12-C14-C18	119.2407	119.2441	118.6878
C12-C14-H19	119.6714	H19-C14-C12	120.6411	120.3731	121.635
C18-C14-H19	120.1375	H19-C14-C18	120.116	120.3804	119.6744
C18-C16-C13	120.3253	C13-C16-C18	119.3578	119.3428	118.8199
C13-C16-H20	119.6276	C13-C16-H20	120.6205	120.373	121.631
C18-C16-H20	120.0462	C18-C16-H20	120.0206	120.2831	119.5475
C14-C18-C16	119.8309	C14-C18-C16	121.069	121.0496	122.1123
C14-C18-H21	120.1467	C14-C18-X31	119.5765	119.5646	119.0868
C16-C18-H21	120.0193	C16-C18-X31	119.3523	119.3837	118.7987
Dihedral angles (Degrees)		Dihedral angles (Degrees)			
C13-C11-C12-C14	1.8085	C13-C11-C12-C14	1.9184	1.8733	1.8835
C13-C11-C12-H15	-177.8307	C13-C11-C12-H15	-177.7537	-177.7491	-177.7313
C6-C11-C13-C16	-178.3285	C6-C11-C13-C16	-178.215	-178.092	-178.1321
C6-C11-C13-H17	0.5369	C6-C11-C13-H17	0.5108	0.6443	0.6579
C16-C13-C11-C12	-0.9593	C16-C13-C11-C12	! -1.0897	-1.0221	-1.0661
C12-C11-C13-H17	177.9062	H17-C13-C11-C12	177.6361	177.7143	177.7238
C11-C12-C14-C18	-1.2917	C11-C12-C14-C18	-1.255	-1.2732	-1.2636

H19-C14-C12-C11	179.3255	C11-C12-C14-H19	179.2884	179.281	179.3478
H15-C12-C14-C18	178.3412	H15-C12-C14-C18	178.4139	178.3457	178.3465
H15-C12-C14-H19	-1.0415	H15-C12-C14-H19	-1.0427	-1.1	-1.0421
C11-C13-C16-C18	-0.4068	C18-C16-C13-C11	-0.3785	-0.4053	-0.3366
C11-C13-C16-H20	179.2647	H20-C16-C13-C11	179.2375	179.2074	179.1992
H17-C13-C16-C18	-179.2757	C18-C16-C13-H17	-179.1192	-179.1567	-179.1375
H17-C13-C16-H20	0.3958	H20-C16-C13-H17	0.4968	0.456	0.3983
C12-C14-C18-C16	-0.1006	C16-C18-C14-C12	-0.2691	-0.2082	-0.2021
C12-C14-C18-H21	-179.4629	C12-C14-C18-X31	-179.7217	-179.6716	-179.6531
H19-C14-C18-C16	179.2793	H19-C14-C18-C16	179.1905	179.2375	179.1988
H19-C14-C18-H21	-0.083	H19-C14-C18-X31	-0.2622	-0.2258	-0.2522
C13-C16-C18-C14	0.9501	C13-C16-C18-C14	1.0807	1.0417	0.9982
C13-C16-C18-H21	-179.6868	C13-C16-C18-X31	-179.4654	-179.494	-179.5494
H20-C16-C18-C14	-178.7201	H20-C16-C18-C14	-178.5376	-178.5714	-178.5475
H20-C16-C18-H21	0.643	H20-C16-C18-X31	0.9162	0.8929	0.905

## 2.2. Optical and electrochemical properties

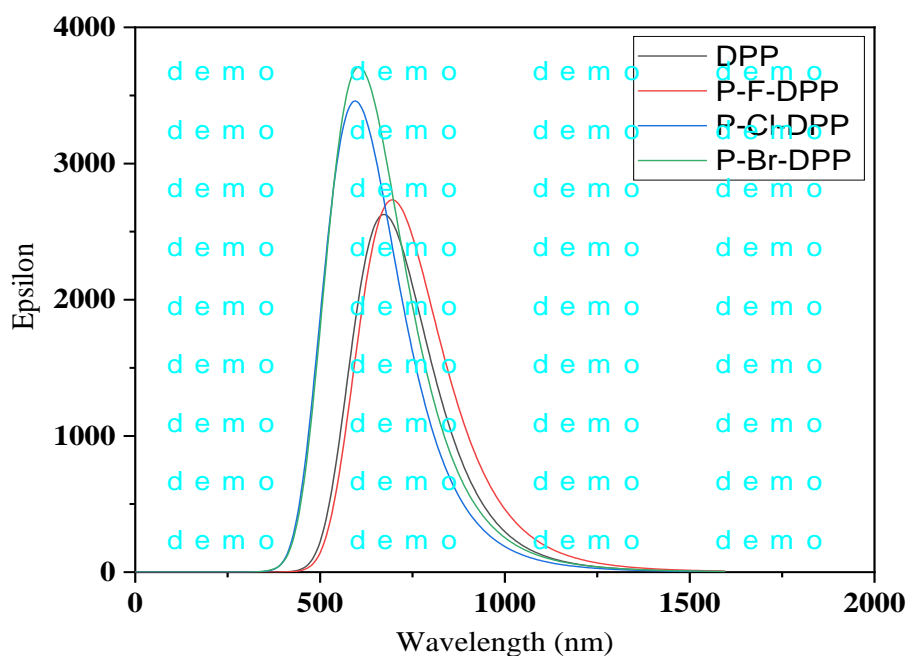
The Time-dependent (TD-DFT/B3LYP) approach was used to determine the entire UV–VIS absorption spectra of the compounds under study at the B3LYP optimised geometry. Recently, time-dependent density functional approaches have emerged as a useful and reasonably reliable tool for single point electronic excitation computations in a variety of molecular systems, specifically conjugated ones [37]. The optical absorbance of all compounds was evaluated in the gas phase, as shown in Figure 3. The estimation of the optical band gap determined from the absorption spectra are 1.8455, 1.7884, 1.7604 and 1.7863eV for DPP, p-Cl DPP p-Br DPP and p-F DPP respectively. The spectral properties of the diphenyl-diketopyrrolopyrrole and its derivatives are compared in Figure 3 the diphenyl-diketopyrrolopyrrole absorption bands range between 500 nm to 850 nm, Cl-DPP showed absorption band in the visible region from 500–900nm, Br-DPP absorption band in the range 500-900nm, F-DPP absorption band in the visible region from 500–900nm. The absorption spectra show red shifted about 50 nm when comparing diphenyl-DPPs with its derivatives. The semiconducting properties of DPP, Cl-P-DPP, Br-P-DPP, and F-P-DPP in gas phase are shown theoretically in Table 3.

Through the UV-visible spectrum results showed the DPP molecule can work as semiconductors in their own right without being included into other derivative materials, but the addition of halogens leads to an increase in its semiconductor properties and also leads to its use in broader fields, as mentioned in the introduction.



**Table 3.** The calculation UV-visible absorption wavelength, excitation energy and oscillator strength of DPP and its derivatives.

Species	The calculated with TD-DFT / B3LYP-6-311G(d,p) in gas phase				
	Wave length (nm)	Energy (eV)	oscillator strength	Major contribution HOMO→LUMO	Transition
DPP	671.83	1.8455	0.0644	92%	$\pi^* \rightarrow \pi$
Cl-P-DPP	693.27	1.7884	0.0847	93%	$\pi^* \rightarrow \pi$
Br-P-DPP	704.30	1.7604	0.0906	93%	$\pi^* \rightarrow \pi$
F-P-DPP	694.09	1.7863	0.0668	92.9%	$\pi^* \rightarrow \pi$

**Figure 3:** UV- UV-VIS absorption spectra of DPP and its derivatives.

### 2.3 Frontier Molecular Orbitals (FMO) Analysis

Descriptors of global reactivity were analysed to comprehend the connection between global chemical reactivity, structure and stability [38]. The frontier molecular orbitals (FMO) called highest occupied molecular orbital (HOMO) and lowest unoccupied molecular orbital (LUMO). The eigenvalues of HOMO and LUMO, as well their energy gap, represents the molecule biological activity. A molecule with a short FMO's gap ( $\Delta E_{LUMO-HOMO}$ ) is more polarisable and has strong chemical reactivity but a low kinetic stability, and vice versa [39]. The ionisation potential is proportional to energy of (HOMO), that can be considered as the

outer orbital housing electrons. However, the LUMO is electron-accepting, and the LUMO energy proportional to the electron affinity [39]. FMOs have significant roles in quantum chemistry, optical, and electrical properties [40]. Figure 4 displays the 3D representations of specific molecular orbitals and the corresponding energy gap for each electronic transition. The (HOMO) exhibits localization throughout the entire molecule, whereas the (LUMO) is primarily localised over the diketopyrrolopyrrole and a limited number of phenyl rings. The disparity existing between these entities corresponds to the quantum energy necessary for the stimulation of an electron's transition from (HOMO) to (LUMO), and is equivalent to chemical hardness [38]. The determination of the (HOMO and LUMO) of compounds serves as a valuable tool for predicting the likelihood of noncovalent interactions within those compounds. Ideally, (HOMO) and the (LUMO) should originate from distinct molecules to ensure a favourable interaction [41]. The ionisation energy and electron affinity may be calculated from the HOMO and LUMO orbital energies as:  $I = -E_{\text{HOMO}}$ ,  $A = -E_{\text{LUMO}}$  [38]. For the **DPP**, has a low value of  $E_{\text{HOMO}} = -6.6\text{eV}$ ,  $E_{\text{LUMO}} = -4.2\text{eV}$  than the **Cl-P-DPP**, **Br-P-DPP** and **F-P-DPP** that have  $E_{\text{HOMO}} = -6.77$ ,  $-6.7$  and  $-6.68\text{eV}$ ,  $E_{\text{LUMO}} = -4.47$ ,  $-4.46$  and  $-4.37\text{eV}$ , energy gap =  $E_{\text{LUMO}} - E_{\text{HOMO}} = 1.8455\text{ eV}$  more than the **Cl-P-DPP**, **Br-P-DPP** and **F-P-DPP** are 1.7884, 1.7604 and 1.7863 eV, ionization potential  $I = 6.6\text{eV}$  and electron affinity  $A = 4.2\text{eV}$ , has a value less than the **Cl-P-DPP**, **Br-P-DPP** and **F-P-DPP** that have ionization potential  $I = 6.77$ , 6.7 and 6.68eV, electron affinity  $A = 4.47$ , 4.46 and 4.37eV, respectively.

The indices of absolute hardness ( $\eta$ ) and softness ( $S$ ) play a crucial role in assessing the stability and reactivity of a molecule [41]. A molecule with high hardness exhibits a significant energy difference between its (HOMO) and (LUMO), while a molecule with low hardness displays a comparatively lower energy gap between these orbitals. Soft molecules exhibit higher reactivity compared to hard molecules due to their enhanced ability to readily transfer the electrons to acceptor [42]. As shown in Table 4, **DPP** has a value of  $\eta$  is (1.2 eV) higher than **Cl-P-DPP**, **Br-P-DPP** and **F-P-DPP** (1.15, 1.12 and 1.155 eV) respectively, whereas **Cl-P-DPP**, **Br-P-DPP** and **F-P-DPP** have a higher  $S$  value (0.434, 0.446 and 0.432 eV) than **DPP** is (0.416 eV). These findings are compatible with the band gap energies of **Cl-P-DPP**, **Br-P-DPP**, and **F-P-DPP** which exhibit smaller band gap energy than **DPP**, they are more reactive (they tend to donate electrons).

Intermolecular and intramolecular reorganisation energies influence the electrochemically-derived HOMO and LUMO energies. Both are caused by ionisation, although the former is due to the rearrangement of solvent shells while the latter is due to modifications to molecule geometry [43]. Descriptors of a molecule's global chemical reactivity can be calculated from its HOMO and LUMO energies [44] Chemical potential energy ( $\mu$ ) refers to a functional group's, atom's, or molecule's tendency to pull electrons (electron density) towards itself in order to react. In essence, a higher value of chemical potential ( $\mu$ ) signifies more difficult for molecule to interaction. Electronegativity ( $\chi$ ) is a fundamental property in chemistry that characterises an atom's affinity for attracting electrons and undergoing anionic transformation. It serves as a quantitative indicator of the chemical reactivity of a given constituent. As the value of  $\chi$  for an atom increases, there is a corresponding increase in the attraction exerted on

electrons towards that atom [45]. The electrophilicity index ( $\omega$ ) quantifies the electrophilic nature of a monomer [38]. Based on values of  $\chi$ ,  $\mu$  and  $\omega$  in Table 3, **DPP** is more reactive than its derivatives, this is because the values of  $\chi$ ,  $\mu$  and  $\omega$  for **DPP** are 5.4, -5.4, and 12.15 eV. compared to the values for **Cl-P-DPP**, which are 5.62, -5.62 and 13.73 eV, **Br-P-DPP** are 5.58, -5.58 and 13.90 eV and **F-P-DPP** are 5.525, -5.525 and 13.21 respectively.

The negative chemical potential seen in diphenyl-diketopyrrolopyrrole and its derivatives indicates the stability of the molecule. Spontaneous decomposition into their constituent parts does not occur. The concept of hardness refers to the ability of chemical systems to resist deformation of their electron cloud when subjected to tiny perturbations during chemical processes [46]. Charge transport is critical in the creation of hydrogen bonds. As a result, the maximum charge transfer ( $N$ ) for DPP and its derivatives was determined to evaluate a monomer's selectivity to operate as an electron acceptor or electron donor.  $\Delta N$  was obtained from equation 1 [42].

$$\Delta N = -\frac{\mu^2}{\eta} \quad \dots\dots\dots (1)$$

$$\mu = -\frac{1}{2}(I + A) \text{ or } \mu = (E_{\text{HOMO}} + E_{\text{LUMO}})/2 \quad \dots\dots\dots (2)$$

$$\eta = \frac{1}{2}(I - A) \text{ or } \eta = (-E_{\text{HOMO}} + E_{\text{LUMO}})/2 \quad \dots\dots\dots (3)$$

$$\chi = (I + A)/2 \quad \dots\dots\dots (4)$$

$$s = 1 / 2\eta \quad \dots\dots\dots (5)$$

$$\omega = \mu^2 / 2\eta \quad \dots\dots\dots (6)$$

Where  $I$  and  $A$  are the ionization potential and electron affinity for the molecules respectively. The parameters results of global chemical reactivity are listed in Table3 [37,39].

**Table 4.** Calculated LUMO ( $E_L$ ) and HOMO ( $E_H$ ) energies, energy gap, global softness ( $S$ ), global hardness ( $\eta$ ), electronegativity ( $\chi$ ), chemical potential ( $\mu$ ), global electrophilicity index ( $\omega$ ), additional electronic charge ( $-\mu/\eta$ ) and the maximum charge transfer ( $\Delta N$ ) for all compounds in gas phase using B3LYP/6-311G(d,p).

	$E_L$ [eV]	$E_H$ [eV]	$E_g$ [eV]	$S$ [eV]	$\eta$ [eV]	$\chi$ [eV <sup>-1</sup> ]	$\mu$ [eV]	$\omega$ [eV]	$-\mu/\eta$	$\Delta N$ [eV]
DPP	-4.2	-6.6	2.39	0.416	1.2	5.4	-5.4	12.15	4.5	-24.3
Cl-P-DPP	-4.47	-6.77	2.3	0.434	1.15	5.62	-5.62	13.73	4.88	-27.46
Br-P-DPP	-4.46	-6.7	2.26	0.446	1.12	5.58	-5.58	13.90	4.98	-27.80
F-P-DPP	-4.37	-6.68	2.3	0.432	1.155	5.525	-5.525	13.21	4.78	-26.429

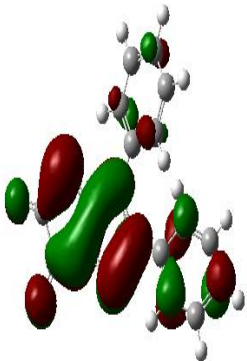
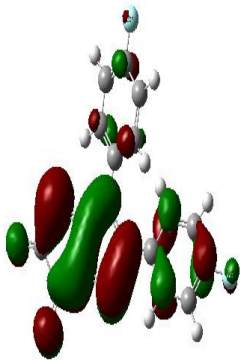
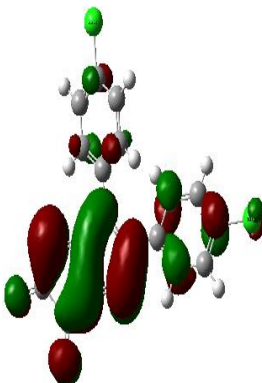
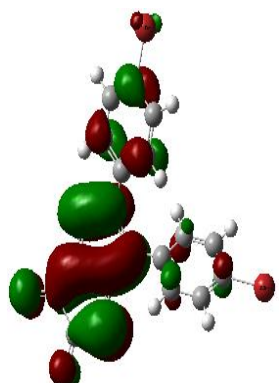
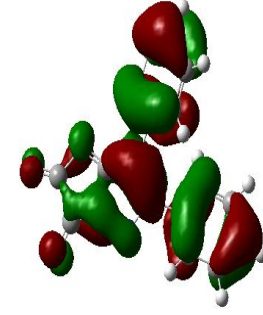
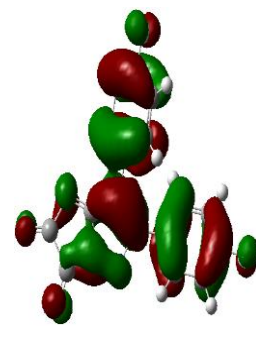
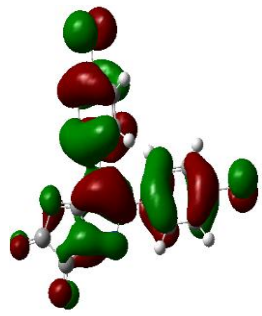
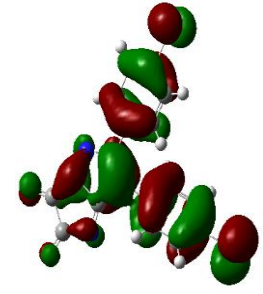
	DPP	F-P-DPP	Cl-P-DPP	Br-P-DPP
LUMO	 $E_{LUMO} = -4.234 \text{ eV}$	 $E_{LUMO} = -4.372 \text{ eV}$	 $E_{LUMO} = -4.473 \text{ eV}$	 $E_{LUMO} = -4.462 \text{ eV}$
HOMO	 $E_{HOMO} = -6.629 \text{ eV}$	 $E_{HOMO} = -6.688 \text{ eV}$	 $E_{HOMO} = -6.775 \text{ eV}$	 $E_{HOMO} = -6.724 \text{ eV}$

Figure 4. Molecular orbitals energies.

### 3. Conclusions

In the present study, the molecular structure and UV-visible spectral of diphenyl-diketopyrrolopyrrole with its derivatives (chlorodiphenyl-diketopyrrolopyrrole, bromodiphenyl-diketopyrrolopyrrole and fluorodiphenyl-diketopyrrolopyrrole) have been calculated using the DFT/B3LYP/6-311G (d,p) level of theory in gas phase. The theoretical results that were available were compared to experimental data gathered from the literature. The computational structural and geometric parameters correlate well with the experimental

ones derived from the literature. Our UV-visible spectrum results reveal that DPP can work as semiconductors in their own right without being included into other derivative materials, however that halogen derivatives improve mobility and charge transfer. On optimised compound structures, frontier molecular orbital analyses (HOMO and LUMO energies) and global chemical reactivity descriptors were derived.

## References

- [1] S. Qu and H. Tian, "Diketopyrrolopyrrole (DPP)-based materials for organic photovoltaics," *Chem. Commun.*, vol. 48, no. 25, pp. 3039–3051, 2012, doi: 10.1039/c2cc17886a.
- [2] N. O. Tapabashi, K. M. Al-janaby, and S. A. Mohammed, "Thermal Performance , Photostability and UV-Visible Spectroscopic Studies of Some Synthesized azo- Schiff and Bis-azo-Schiff bases," no. 7, pp. 210–212, 2017.
- [3] A. M. Ghaleb and A. Q. Ahmed, "Structural, electronic, and optical properties of sphalerite ZnS compounds calculated using density functional theory (DFT)," *Chalcogenide Lett.*, vol. 19, no. 5, pp. 309–318, May 2022, doi: 10.15251/CL.2022.195.309.
- [4] N. Mohammed, S. J. Shakkor, S. M. Abdalhadi, and Y. K. Al-Bayati, "Two multifunctional benzoquinone derivatives as small molecule organic semiconductors for bulk heterojunction and perovskite solar cells," *Main Gr. Chem.*, vol. 21, no. 4, pp. 943–952, Dec. 2022, doi: 10.3233/MGC-210187.
- [5] Q. Liu, S. E. Bottle, and P. Sonar, "Developments of Diketopyrrolopyrrole-Dye-Based Organic Semiconductors for a Wide Range of Applications in Electronics," *Adv. Mater.*, vol. 32, no. 4, pp. 1–46, 2020, doi: 10.1002/adma.201903882.
- [6] R. Almughathawi, S. Hou, Q. Wu, Z. Liu, W. Hong, and C. Lambert, "Conformation and Quantum-Interference-Enhanced Thermoelectric Properties of Diphenyl Diketopyrrolopyrrole Derivatives," *ACS Sensors*, vol. 6, no. 2, pp. 470–476, 2021, doi: 10.1021/acssensors.0c02043.
- [7] Q. Yang, X. Sun, J. Han, and L. Wang, "Beauty in chemistry: A self-organized and dual-phase emissive diketopyrrolopyrrole derivative as high-yield fluorescent material," *Dye. Pigment.*, vol. 194, no. July, p. 109655, 2021, doi: 10.1016/j.dyepig.2021.109655.
- [8] Q. Liu, S. E. Bottle, and P. Sonar, "Developments of Diketopyrrolopyrrole-Dye-Based Organic Semiconductors for a Wide Range of Applications in Electronics," *Adv. Mater.*, vol. 32, no. 4, 2020, doi: 10.1002/adma.201903882.
- [9] Y. Cai *et al.*, "Small-molecule diketopyrrolopyrrole-based therapeutic nanoparticles for photoacoustic imaging-guided photothermal therapy," *Nano Res.*, vol. 10, no. 3, pp. 794–801, 2017, doi: 10.1007/s12274-016-1332-2.
- [10] X. Wang, B. Jiang, C. Du, X. Ren, Z. Duan, and H. Wang, "Fluorinated dithienyl-diketopyrrolopyrrole: A new building block for organic optoelectronic materials," *New J. Chem.*, vol. 43, no. 41, pp. 16411–16420, 2019, doi: 10.1039/c9nj04060a.
- [11] Z. Yi, S. Wang, and Y. Liu, "Design of High-Mobility Diketopyrrolopyrrole-Based  $\pi$ -



- Conjugated Copolymers for Organic Thin-Film Transistors,” *Adv. Mater.*, vol. 27, no. 24, pp. 3589–3606, 2015, doi: 10.1002/adma.201500401.
- [12] J. Xu *et al.*, “Aryl modification of diketopyrrolopyrrole-based quaternary ammonium salts and their applications in copper electrodeposition,” *Dye. Pigment.*, vol. 170, no. April, p. 107559, 2019, doi: 10.1016/j.dyepig.2019.107559.
- [13] J. Humphreys *et al.*, “Solid state structure and properties of phenyl diketopyrrolopyrrole derivatives,” *CrystEngComm*, vol. 23, no. 8, pp. 1796–1814, 2021, doi: 10.1039/d1ce00039j.
- [14] W. W. Bao *et al.*, “Diketopyrrolopyrrole (DPP)-Based Materials and Its Applications: A Review,” *Front. Chem.*, vol. 8, no. September, pp. 1–6, 2020, doi: 10.3389/fchem.2020.00679.
- [15] M. Raftani, T. Abram, A. Azaid, R. Kacimi, M. N. Bennani, and M. Bouachrine, “Theoretical design of new organic compounds based on diketopyrrolopyrrole and phenyl for organic bulk heterojunction solar cell applications: DFT and TD-DFT study,” *Mater. Today Proc.*, vol. 45, pp. 7334–7343, 2021, doi: 10.1016/j.matpr.2020.12.1228.
- [16] S. M. Wagalgave *et al.*, “Aggregation induced emission (AIE) materials based on diketopyrrolopyrrole chromophore for CdS nanowire solar cell applications,” *J. Electroanal. Chem.*, vol. 895, no. May, p. 115451, 2021, doi: 10.1016/j.jelechem.2021.115451.
- [17] M. Raftani, T. Abram, A. Azaid, R. Kacimi, M. N. Bennani, and M. Bouachrine, “Theoretical design of new organic compounds based on diketopyrrolopyrrole and phenyl for organic bulk heterojunction solar cell applications: DFT and TD-DFT study,” *Mater. Today Proc.*, vol. 45, no. xxxx, pp. 7334–7343, 2021, doi: 10.1016/j.matpr.2020.12.1228.
- [18] B. Barszcz, K. Kędzierski, H. Y. Jeong, and T. D. Kim, “Spectroscopic properties of diketopyrrolopyrrole derivatives with long alkyl chains,” *J. Lumin.*, vol. 185, pp. 219–227, 2017, doi: 10.1016/j.jlumin.2017.01.019.
- [19] Y. Patil and R. Misra, “Rational molecular design towards NIR absorption: Efficient diketopyrrolopyrrole derivatives for organic solar cells and photothermal therapy,” *J. Mater. Chem. C*, vol. 7, no. 42, pp. 13020–13031, 2019, doi: 10.1039/c9tc03640g.
- [20] L. Wang, B. Lai, X. Ran, H. Tang, and D. Cao, “Recent Advances of Diketopyrrolopyrrole Derivatives in Cancer Therapy and Imaging Applications,” *Molecules*, vol. 28, no. 10, 2023, doi: 10.3390/molecules28104097.
- [21] A. Chiminazzo *et al.*, “Diketopyrrolopyrrole Bis-Phosphonate Conjugate: A New Fluorescent Probe for In Vitro Bone Imaging,” *Chem. - A Eur. J.*, vol. 25, no. 14, pp. 3617–3626, 2019, doi: 10.1002/chem.201805436.
- [22] Y. Jiang *et al.*, “Multibranched triarylamine end-capped triazines with aggregation-induced emission and large two-photon absorption cross-sections,” *Chem. Commun.*, vol. 46, no. 26, pp. 4689–4691, 2010, doi: 10.1039/c0cc00803f.
- [23] J. David, M. Weiter, M. Vala, J. Vyňuchal, and J. Kučerík, “Stability and structural aspects of diketopyrrolopyrrole pigment and its N-alkyl derivatives,” *Dye. Pigment.*,

- vol. 89, no. 2, pp. 137–143, 2011, doi: 10.1016/j.dyepig.2010.10.001.
- [24] S. G. Surya, S. S. Nagarkar, S. K. Ghosh, P. Sonar, and V. Ramgopal Rao, "OFET based explosive sensors using diketopyrrolopyrrole and metal organic framework composite active channel material," *Sensors Actuators, B Chem.*, vol. 223, pp. 114–122, 2016, doi: 10.1016/j.snb.2015.09.076.
- [25] M. Vala, J. Vyňuchal, P. Toman, M. Weiter, and S. Luňák, "Novel, soluble diphenyl-diketo-pyrrolopyrroles: Experimental and theoretical study," *Dye. Pigment.*, vol. 84, no. 2, pp. 176–182, 2010, doi: 10.1016/j.dyepig.2009.07.014.
- [26] D. Cao, Q. Liu, W. Zeng, S. Han, J. Peng, and S. Liu, "Diketopyrrolopyrrole-containing polyfluorenes: Facile method to tune emission color and improve electron affinity," *Macromolecules*, vol. 39, no. 24, pp. 8347–8355, 2006, doi: 10.1021/ma0615349.
- [27] Y. Zhu, A. R. Rabindranath, T. Beyerlein, and B. Tieke, "Highly luminescent 1,4-diketo-3,6-diphenylpyrrolo[3,4-c]pyrrole-(DPP-) based conjugated polymers prepared upon suzuki coupling," *Macromolecules*, vol. 40, no. 19, pp. 6981–6989, 2007, doi: 10.1021/ma0710941.
- [28] S. Matsumura *et al.*, "Stability and Utility of Pyridyl Disulfide Functionality in RAFT and Conventional Radical Polymerizations," *J. Polym. Sci. Part A Polym. Chem.*, vol. 46, no. April, pp. 7207–7224, 2008, doi: 10.1002/pola.
- [29] S. Luňák, J. Vyňuchal, and R. Hrdina, "Geometry and absorption of diketo-pyrrolopyrrole isomers and their  $\pi$ -isoelectronic furo-furanone analogues," *J. Mol. Struct.*, vol. 919, no. 1–3, pp. 239–245, 2009, doi: 10.1016/j.molstruc.2008.09.022.
- [30] Y. S. Mary *et al.*, "FT-IR, FT-Raman, SERS and computational study of 5-ethylsulphonyl-2-(o- chlorobenzyl)benzoxazole," *Spectrochim. Acta - Part A Mol. Biomol. Spectrosc.*, vol. 96, pp. 617–625, 2012, doi: 10.1016/j.saa.2012.07.006.
- [31] J. Lukose *et al.*, "Synthesis, structural and vibrational investigation on 2-phenyl-N-(pyrazin- 2-yl)acetamide combining XRD diffraction, FT-IR and NMR spectroscopies with DFT calculations," *Spectrochim. Acta - Part A Mol. Biomol. Spectrosc.*, vol. 135, pp. 608–616, 2015, doi: 10.1016/j.saa.2014.07.004.
- [32] Y. S. Mary *et al.*, "Vibrational spectra, NBO analysis, HOMO-LUMO and first hyperpolarizability of 2-[[2-Methylprop-2-en-1-yl]oxy]methyl}-6-phenyl-2,3,4,5-tetrahydro-1,2,4- triazine-3,5-dione, a potential chemotherapeutic agent based on density functional theory calculations," *Spectrochim. Acta - Part A Mol. Biomol. Spectrosc.*, vol. 133, pp. 449–456, 2014, doi: 10.1016/j.saa.2014.06.036.
- [33] M. Karabacak, M. Çınar, A. Çoruh, and M. Kurt, "Theoretical investigation on the molecular structure, Infrared, Raman and NMR spectra of para-halogen benzenesulfonamides, 4-X-C<sub>6</sub>H<sub>4</sub>SO<sub>2</sub>NH<sub>2</sub> (X = Cl, Br or F)," *J. Mol. Struct.*, vol. 919, no. 1–3, pp. 26–33, 2009, doi: 10.1016/j.molstruc.2008.08.007.
- [34] V. Arjunan and S. Mohan, "Fourier transform infrared and FT-Raman spectral analysis and ab initio calculations for 4-chloro-2-methylaniline and 4-chloro-3-methylaniline," *J. Mol. Struct.*, vol. 892, no. 1–3, pp. 289–299, 2008, doi: 10.1016/j.molstruc.2008.05.053.

- [35] P. K. Murthy *et al.*, "Synthesis, conformational, characterization and reactivity study of 1,7-bis(4-bromophenyl)heptane-1,7-dione," *J. Mol. Struct.*, vol. 1175, pp. 269–279, 2019, doi: 10.1016/j.molstruc.2018.08.003.
- [36] B. T. Gowda, K. Jyothi, J. Kožíšek, and H. Fuess, "Crystal Structure Studies on p-Substitutedbenzenesulphonamides 4-X-C<sub>6</sub>H<sub>4</sub>SO<sub>2</sub>NH<sub>2</sub> (X = CH<sub>3</sub>, NH<sub>2</sub> F, Cl or Br)," *Zeitschrift fur Naturforsch. - Sect. A J. Phys. Sci.*, vol. 58, no. 11, pp. 656–660, 2003, doi: 10.1515/zna-2003-1110.
- [37] M. Vala, M. Weiter, J. Vyňuchal, P. Toman, and S. Luňák, "Comparative studies of diphenyl-diketo-pyrrolopyrrole derivatives for electroluminescence applications," *J. Fluoresc.*, vol. 18, no. 6, pp. 1181–1186, 2008, doi: 10.1007/s10895-008-0370-x.
- [38] E. Normaya, M. N. Ahmad, Y. Farina, and K. H. K. Bulat, "Synthesis, characterization and preliminary study on acetylpyrazine N(4)butylthiosemicarbazone as a potential CDK2 inhibitor combined with DFT calculations," *J. Braz. Chem. Soc.*, vol. 29, no. 10, pp. 2197–2206, 2018, doi: 10.21577/0103-5053.20180097.
- [39] A. Karmakar, P. Bandyopadhyay, S. Banerjee, N. C. Mandal, and B. Singh, "Synthesis, spectroscopic, theoretical and antimicrobial studies on molecular charge-transfer complex of 4-(2-thiazolylazo)resorcinol (TAR) with 3, 5-dinitrosalicylic acid, picric acid, and chloranilic acid," *J. Mol. Liq.*, vol. 299, p. 112217, 2020, doi: 10.1016/j.molliq.2019.112217.
- [40] B. Kosar and C. Albayrak, "Spectroscopic investigations and quantum chemical computational study of (E)-4-methoxy-2-[(p-tolylimino)methyl]phenol," *Spectrochim. Acta - Part A Mol. Biomol. Spectrosc.*, vol. 78, no. 1, pp. 160–167, 2011, doi: 10.1016/j.saa.2010.09.016.
- [41] M. Liu, J. Chen, Y. Chen, and Y. Zhu, "Interaction between smithsonite and carboxyl collectors with different molecular structure in the presence of water: A theoretical and experimental study," *Appl. Surf. Sci.*, vol. 510, no. January, p. 145410, 2020, doi: 10.1016/j.apsusc.2020.145410.
- [42] M. A. Mohammad Alwi *et al.*, "Two-Dimensional Infrared Correlation Spectroscopy, Conductor-like Screening Model for Real Solvents, and Density Functional Theory Study on the Adsorption Mechanism of Polyvinylpolypyrrolidone for Effective Phenol Removal in an Aqueous Medium," *ACS Omega*, vol. 6, no. 39, pp. 25179–25192, 2021, doi: 10.1021/acsomega.1c02699.
- [43] M. Vala and J. Kraj, "Author 's personal copy Dyes and Pigments HOMO and LUMO energy levels of N , N 0 -dinitrophenyl-substituted polar diketopyrrolopyrroles ( DPPs )".
- [44] C. B. Nielsen, M. Turbiez, and I. McCulloch, "Recent advances in the development of semiconducting DPP-containing polymers for transistor applications," *Adv. Mater.*, vol. 25, no. 13, pp. 1859–1880, 2013, doi: 10.1002/adma.201201795.
- [45] N. N. Nyangiwe and C. N. M. Ouma, "Adsorption and coadsorption of single and multiple natural organic matter on Ag (1 1 1) surface: A DFT-D study," *Appl. Surf. Sci.*, vol. 505, no. 111, p. 144609, 2020, doi: 10.1016/j.apsusc.2019.144609.

- [46] R. T. Ulahannan *et al.*, “Molecular structure, FT-IR, FT-Raman, NBO, HOMO and LUMO, MEP, NLO and molecular docking study of 2-[(E)-2-(2-bromophenyl)ethenyl]quinoline-6-carboxylic acid,” *Spectrochim. Acta - Part A Mol. Biomol. Spectrosc.*, vol. 151, pp. 184–197, 2015, doi: 10.1016/j.saa.2015.06.077.